Cooperative Spectrum Sharing Between Cellular and Ad-Hoc Networks

Chao Zhai, *Student Member, IEEE,* Wei Zhang, *Senior Member, IEEE,* and Guoqiang Mao, *Senior Member, IEEE*

***Abstract*—We consider the problem of spectrum sharing between cellular network downlink and ad-hoc network coexisting in the same region. The weak signal and strong interference at cell-edge area often cause difficulty in guaranteeing the quality of service requirement. To improve the spectrum efficiency and cell-edge link quality, we propose a cooperative spectrum sharing scheme. The ad-hoc users can actively help the base station with its data transmission to improve the average throughput of cellular network downlink. As a reward, a fraction of cellular network spectrum can be released to the ad-hoc network for its own data transmission. We aim to maximize the ad-hoc transmission capacity subject to the constraints on the outage probability of ad-hoc network and on the throughput improvement ratio of cellular network. Both the transmission capacity of ad-hoc network and the average throughput of cellular network are analyzed using the stochastic geometry theory. The optimal ad-hoc user density and spectrum allocation are calculated through solving an optimization problem. Numerical and simulation results are provided to validate our theoretical analysis and show the impacts of system parameters. It demonstrates that our proposed scheme can effectively facilitate ad-hoc transmissions while moderately improving the cellular network performance.**

***Index Terms*—Cognitive radio, cooperative diversity, spectrum sharing, stochastic geometry, transmission capacity.**

I. Introduction

Cognitive spectrum sharing has recently been intensively studied to accommodate the growing demand for wireless broadband access, which can alleviate the problem of underutilization of licensed spectrum. The spectrum sharing techniques can be classified into three categories: interweave, underlay, and overlay [1]. For the interweave spectrum sharing, the secondary system can opportunistically access the spectrum holes, while for the underlay scheme, the secondary users (SUs) transmit simultaneously with primary users (PUs) under the constraint that interference caused by SUs on PUs must be below a certain threshold. For the overlay scheme, the SUs actively help the primary data transmission in exchange for the spectrum access in time domain [2], spatial domain [3], or frequency domain [4]. The locations of SUs are usually fixed or restricted into a small area without suffering interference from other concurrent links. It is nontrivial to extend the cooperative spectrum sharing to the secondary ad-hoc networks, as the topology changes frequently and the interference suffers from uncertainties caused by both random user locations and channel fadings.

C. Zhai and W. Zhang are with the School of Electrical Engineering and Telecommunications, The University of New South Wales, Sydney, Australia (e-mail: chao.zhai@student.unsw.edu.au; wzhang@ee.unsw.edu.au).

G. Mao is with the School of Electrical and Information Engineering, The University of Sydney, Sydney, Australia (e-mail: guoqiang.mao@sydney.edu.au).

A. Related Work and Motivation

Transmission capacity has often been used as a major performance metric to study ad-hoc networks and it represents the area spectral efficiency constrained by the outage probability [5]. Through modeling users' locations as homogeneous Poisson Point Process (PPP) in the overlaid spectrum sharing system, Huang *et al.* studied the transmission capacity tradeoff between primary system and secondary system [6]. Lee *et al.* developed a comprehensive framework with multiple systems and studied the transmission capacity under the constraints of both outage probability and fair coexistence [7]. Yin *et al.* studied the impacts of mutual interference between primary and secondary systems and found that a slight degradation of the primary outage probability can lead to a significant increase of the total transmission capacity [8]. The underlay spectrum sharing is realized in [9] by applying an exclusive region [10] around the single primary link such that the SU transmission is prohibited in the region. For the cognitive radio network with multiple primary links, the active SUs form the Poisson hole process due to the exclusive regions, and the approximate outage probability is derived in [11]. For the interweave spectrum sharing, the impacts of spectrum sensing to the primary transmission are revealed by analyzing the characteristics of the aggregate interference [12]– [14]. The stochastic geometry models of three types of cognitive radio networks are proposed in [15], where the single primary link, multicast primary system, or primary ad-hoc network coexists with a secondary ad-hoc network operating with the carrier sense multiple access (CSMA) protocol.

Cooperative communications can significantly enhance the performance of wireless systems by exploiting the spatial diversity [16]. Most of the literatures about cooperation focus on a fixed network topology [17] [18], where the users' locations are unchanged. Wang *et. al.* studied the decode-and-forward (DF) cooperation with best relay selection, where the relays are randomly distributed on the plane following PPP. A spatial quality of service (QoS) region around the source and destination link is applied in [19] to reduce the overhead and latency in the best relay selection. To further reduce the excessive overhead in the coordination phase, the uncoordinated cooperation protocols are proposed assuming the PPP distribution of relay nodes [20] [21]. In terms of transmission capacity, the DF based incremental relaying or selection cooperation [22] significantly outperforms the non-cooperative system as shown in [23] [24].

In cognitive radio networks with users randomly distributed, the existing literatures mainly focus on the non-cooperative un-

derlay and interweave spectrum sharing. The spectrum access of the secondary system can only degrade the performance of the primary system and will not bring any contribution to the primary system. This motivates us to study the effect of overlay spectrum sharing, where the SUs actively help the PUs with their transmissions in exchange for some spectrum release by the primary system for the secondary data transmission. However, it is a challenging issue to study the performance of an overlay spectrum sharing system, as the interferences encountered at both the relay and the receiver are dependent. Ganti *et al.* have studied the two-hop communication with relay selection to mitigate the dead-zone in the cell-edge area of the cellular network [25]. In their work, the success probability of the two-hop system is analyzed with the base stations (BSs) placed on a regular grid, which is too ideal to model the upcoming heterogenous networks [26]. To capture the increasingly random and dense placement of BSs in future networks [27], it is more practical to model the BSs as a random spatial point process. Compared with the cellular network uplink [6], the downlink bandwidth is much broader and its data traffic is much heavier, so the spectrum efficiency can be further improved by sharing the downlink spectrum as focused on in our work.

B. Contribution and Organization

In this work, we focus on modeling and analyzing the cooperative spectrum sharing between cellular network downlink and ad-hoc network. The cellular network is the primary system that owns the licensed spectrum, while the ad-hoc network is the secondary system. The same spectrum is reused among different cells and the interference exists over the primary data transmission. In the cellular network, the cell-edge communication is a bottleneck to guarantee the overall QoS requirement, because the desired signal is relatively weak compared with the interference [27]. To improve the quality of cell-edge communication, we apply a cooperation region between each BS and its cell-edge mobile user (MU). The SU in the cooperation region that can correctly decode the primary data and has the best channel state towards the cell-edge MU is selected for the data retransmission in case the original transmission fails. As a reward of the cooperation, a fraction of spectrum is released to the secondary system and the remaining bandwidth is kept by the primary system. Using the stochastic geometry theory, we analyze the transmission capacity of ad-hoc network and the average throughput of cellular network downlink. The optimal bandwidth allocation is obtained through maximizing the secondary transmission capacity subject to the constraints of secondary outage probability and primary throughput improvement ratio. Numerical and simulation results are provided to show the impacts of system parameters and verify the efficiency of our proposed scheme.

The rest of this paper is organized as follows. In Section II, the system model is introduced. Section III formulates the optimization problem and obtains the secondary transmission capacity. Section IV derives the average throughput of primary downlink based on the analysis of success probabilities. The optimal SU density and bandwidth allocation are calculated in Section V. Numerical and simulation results are presented in Section VI. Section VII concludes this paper.

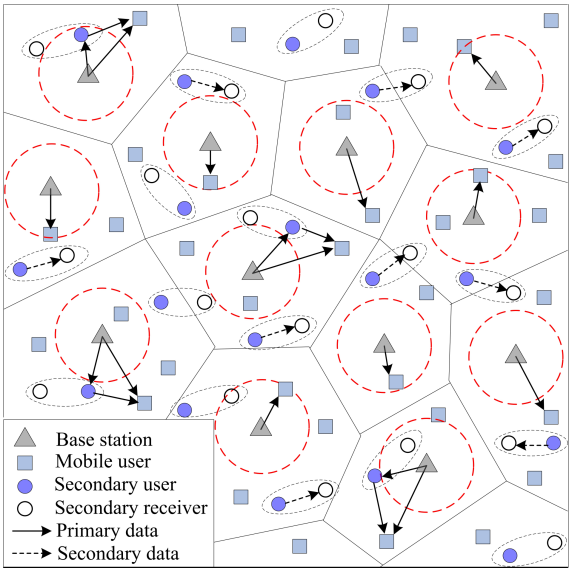

Fig. 1. The overlaid wireless network with PPP modeling for both systems. Each mobile user (MU) is associated with its nearest base station (BS), so the *Voronoi* cell is formed in the cellular network. The circular area around each BS represents the cell-interior area, with radius c_0. In each *Voronoi* cell, the outside of the circular area represents the cell-edge area. The potential secondary users (SUs) in each cell can actively help the cell-edge downlink communications in exchange for a fraction of disjoint spectrum band. Each SU has a fixed receiver departed d meters away, and they are paired together by the ellipse. The Aloha-type protocol is implemented in the ad-hoc network to activate the SUs to access the released disjoint spectrum band.

II. System Description

The licensed spectrum belongs to the cellular network and it is reused by different cells. The locations of BSs and MUs are modeled as two independent homogenous PPPs $\Pi_{\rm b} = \{x_i, i \in \mathbb{Z}\}$ and $\Pi_{\rm m} = \{y_i, i \in \mathbb{Z}\}$ with intensities $\lambda_{\rm b}$ and $\lambda_{\rm m}$, respectively. Each MU is served by its nearest BS. As plotted in Fig. 1, the cellular network forms a *Poisson Tessellation* of the plane and each cell is known as a *Voronoi* cell [6]. Each BS communicates with one randomly selected MU in its cell and the downlink communication is studied. An ad-hoc network is overlaid with the cellular network and it forms the secondary system. The locations of SUs follow another PPP with intensity $\lambda_{\rm s}$, i.e., $\Pi_{\rm s} = \{z_i, i \in \mathbb{Z}\}$. Each SU has a receiver departed d meters away. This assumption may be easily relaxed but at the cost of complicating the derived expressions without providing additional insight [5], as picking the distance d from a random distribution only reduces the transmission capacity by a constant factor [28]. The Aloha-type protocol is adopted in the ad-hoc network to control the channel access of SUs. Whether a SU could access the channel or not is determined by the media access probability (MAP) $\xi \in (0, 1)$. The channel between any pair of terminals u_1 and u_2 undergoes small-scale block fading and large-scale path-loss. The power fading G_{u_1,u_2} is exponentially distributed with unit mean, and it is independent across links. The path-loss is $\ell_{u_1,u_2}^{-\alpha}$, where $\ell_{u_1,u_2} = |u_1 - u_2|$ is the distance and α

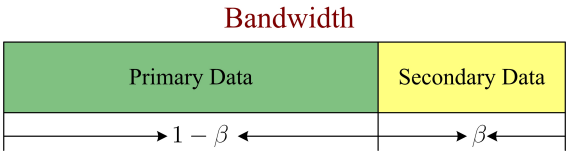

Fig. 2. Bandwidth division between primary and secondary systems. The fraction β is released to the secondary system, while the remaining $1-\beta$ fraction is kept by the primary system for the direct or cooperative data transmission.

is the path-loss exponent. The symbol u_2 in the subscript is omitted for brevity if u_2 lies at the origin. The interference-limited environment is considered and the effect of noise is neglected.

A. Spectrum Sharing Model

We consider the overlay spectrum sharing, where a fraction of spectrum is released to the ad-hoc network in exchange for its cooperation for the cell-edge communication [4]. Without loss of generality, the total bandwidth is set as unit and the spectrum released to the secondary system is $\beta \in (0,1)$, while the remaining $1-\beta$ fraction of spectrum is reserved by the primary system as shown by Fig. 2. The primary system and secondary system do not interfere with each other as disjoint frequency bands are utilized.

If the randomly selected MU lies at the cell-interior of its serving BS, the direct transmission is performed, because the channel is usually good and the interference is relatively weak. The bandwidth release may be tolerated by the primary downlink. The interior area is defined as a circular area centered at the BS with radius c_0. However, if the MU lies at the cell-edge of its serving BS, cooperative communications are employed. With the cooperation from SUs, the throughput of primary data transmission can be enhanced to combat the strong interference. Moreover, the benefits of cooperation can be exploited to combat the negative effect of spectrum release. The more spectrum is released, the higher capacity is achieved for the secondary system. However, less capacity is retained for the primary system due to the remaining narrower bandwidth. Therefore, the bandwidth allocation should be judiciously determined to maximize the secondary capacity without violating the primary performance requirement in the cooperative spectrum sharing.

B. Cooperation Model

The truncated automatic repeat request (ARQ) scheme with one-time retransmission is adopted for the communication between BS and its cell-interior MU. If the original transmission is successful, the acknowledgement (ACK) frame is fed back and the BS continues to transmit a new data packet. Otherwise, the negative acknowledgement (NACK) frame is released and the BS retransmits the same data packet. The received signals in both the original and the retransmission phases are maximal ratio combined (MRC) by the cell-interior MU for the detection.

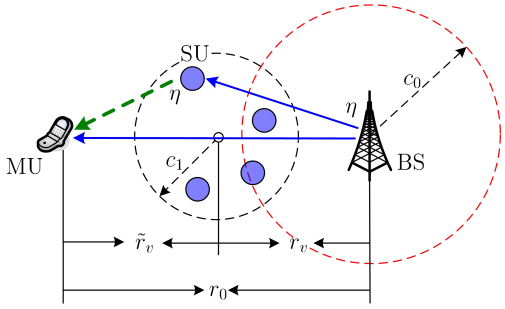

Fig. 3. The cooperation model for the cell-edge MU. The corresponding receiver for each SU is not plotted in this figure.

The existing cooperative truncated ARQ scheme based on DF protocol [29], which is also known as the DF based incremental relaying [22], is adopted to assist the data transmission between the BS and its cell-edge MU. As shown in Fig. 3, a cooperation region is applied between the BS and its cell-edge MU, which can be designated by the BS through a handshake process or determined automatically by each SU using its estimated location obtained from the localization technique [30]. The distance between BS and the center of cooperation region is denoted as $r_v = \zeta r_0$ with $0 < \zeta < 1$, while the distance between the center of cooperation region and the cell-edge MU is $\tilde{r}_v = (1-\zeta) r_0$. The SUs in the cooperation region will help the primary data transmission. In the original phase, the BS broadcasts its data to the intended cell-edge MU and all the SUs in the cooperation region. The SUs that can correctly decode the original primary data are called *decoding SUs*. Three cases will occur according to whether the MU and the SUs correctly receive the primary data or not.

- Case I: The cell-edge MU correctly receives the data packet, and the ACK frame is broadcast. The SUs in the cooperation region refresh their memories and the BS continues to transmit a new data packet.
- Case II: The cell-edge MU erroneously receives the primary data and the NACK frame is fed back. There are no SUs or no decoding SUs in the cooperation region. In this case, the BS retransmits its original data and all the SUs in the cooperation region keep silent.
- Case III: The cell-edge MU erroneously receives the primary data and the NACK frame is released. There exists at least one decoding SU in the cooperation region and the one with best channel state towards the cell-edge MU retransmits. The best decoding SU can be selected in a distributed way using the time back-off [17] or signaling burst scheme [31]. When the selected SU performs the retransmission, the BS together with all the other SUs in the cooperation region will keep silent.

We assume that the control frame sent by the MU can be reliably received by both the BS and the relaying SUs. The channel coefficient is assumed to be available for each receiver to coherently detect signals. Each decoding SU can estimate its channel state towards the cell-edge MU through measuring the NACK frame. When the original cell-edge transmission fails, only one decoding SU or the BS is activated for the signal retransmission. Through using the control frame and the

distributed coordination scheme [17] [31], we can determine which case will occur and whether a SU is involved in the retransmission. The retransmission is performed by the SU only in Case III, where the decoding SU with the best channel quality towards the cell-edge MU is activated to forward the BS signal. The original and retransmitted signals are maximal ratio combined by the cell-edge MU in the time domain for the coherent detection.

III. Transmission Capacity of Secondary System

We aim to maximize the transmission capacity [5] of secondary system while satisfying the primary performance requirement. The optimization problem is formulated as

$$\max_{\lambda_\mathrm{s}>0,\,0<\beta<1} \quad C_\mathrm{s}^\epsilon = \xi\lambda_\mathrm{s}(1-\epsilon)T_1 \tag{1}$$

$$\text{s. t.} \quad P_\mathrm{out}^\mathrm{s}(\lambda_\mathrm{s},\beta) \le \epsilon \tag{2}$$

$$\frac{V_\mathrm{c}(\lambda_\mathrm{s},\beta)-V_\mathrm{d}}{V_\mathrm{d}} \ge \rho, \tag{3}$$

where C_s^ϵ is the transmission capacity of secondary system. The transmission rate of each secondary link is assumed to be the same and it is denoted as T_1. The outage probability $P_\mathrm{out}^\mathrm{s}(\lambda_\mathrm{s},\beta)$ of each secondary link should be no larger than the target outage probability ϵ. The average throughput of primary system with and without cooperative spectrum sharing is denoted as $V_\mathrm{c}(\lambda_\mathrm{s},\beta)$ and V_d, respectively. The parameter $\rho \ge 0$ represents the required throughput improvement ratio of the primary downlink introduced by the cooperative spectrum sharing. The optimal SU density λ_s and the optimal bandwidth allocation factor β are investigated for the optimization problem.

Since SUs transmit according to an Aloha-type protocol [31], the simultaneous transmitting SUs form a homogeneous PPP $\tilde{\Pi}_\mathrm{s}$ with density $\xi\lambda_\mathrm{s}$, which is obtained through an independent thinning of Π_s. Without loss of generality, we consider and evaluate the performance of a typical secondary receiver located at the origin. According to Slivnyak's theorem [32], this artificial placement does not affect the distribution of other users. The achievable rate of secondary data transmission is given as

$$R_\mathrm{s} = \beta\log_2\Big(1+\frac{G_{z_0}d^{-\alpha}}{\mathcal{I}_\mathrm{s}}\Big), \tag{4}$$

where G_{z_0} is the small-scale power fading. The pre-factor β is applied in (4) due to the division of bandwidth for the spectrum sharing. The interference term in (4) is expressed as

$$\mathcal{I}_\mathrm{s} = \sum_{z\in\tilde{\Pi}_\mathrm{s}/\{z_0\}} G_z\ell_z^{-\alpha}, \tag{5}$$

where all the active SUs except the typical one contribute to the aggregate interference. The outage probability of this typical secondary link is derived as [33],

$$\begin{aligned} P_\mathrm{out}^\mathrm{s}(\lambda_\mathrm{s},\beta) &= \mathbb{P}\big\{R_\mathrm{s}<T_1\big\} = \mathbb{P}\big\{G_{z_0}<\tau_1 d^\alpha\mathcal{I}_\mathrm{s}\big\} \\ &= 1-\exp\left[-\xi\lambda_\mathrm{s}\pi\tau_1^{\frac{2}{\alpha}}d^2\frac{2\pi/\alpha}{\sin(2\pi/\alpha)}\right], \end{aligned} \tag{6}$$

where $\tau_1 = 2^{T_1/\beta}-1$ with T_1 denoting the target rate of secondary system.

Remarks: (1) The increase of β leads to the decrease of τ_1. With the decrease of τ_1, the outage probability gets smaller. Therefore, the higher bandwidth allocation is beneficial to support the secondary transmission and hence reduce the outage probability. But, the primary performance gets worse with the increase of β, so we hope to find a trade-off of this parameter. (2) The outage performance gets worse with the increase of SU density λ_s, because the more concurrent secondary transmissions, the stronger the interference and hence the worse the performance.

IV. Average Throughput of Primary System

In this section, we first introduce the distribution of the random distance between a BS and its intended MU. The aggregate interference encountered at the typical MU is approximated. Then, we analyze the success probabilities for the cell-interior and cell-edge communications. Finally, the average throughput of the cellular network downlink is derived.

A. Distance Distribution and Interference Model

One typical MU is located at the origin and the typical MU is served by its nearest BS located at x_0. Their distance is denoted as r_0, which is a realization of the random variable R (the random distance between a BS and its intended MU in the serving area). The complementary cumulative distribution function (CCDF) is given as [26]

$$\begin{aligned} \Pr\{R>r_0\} &= \Pr\{\text{No BS closer than } r_0\} \\ &= \exp(-\lambda_\mathrm{b}\pi r_0^2). \end{aligned} \tag{7}$$

Then, the cumulative distribution function (CDF) is obtained as $F_R(r_0) = 1-\exp(-\lambda_\mathrm{b}\pi r_0^2)$, so the probability density function (PDF) is obtained as

$$f_R(r_0) = \frac{\mathrm{d}F_R(r_0)}{\mathrm{d}r_0} = 2\pi\lambda_\mathrm{b}r_0\exp(-\lambda_\mathrm{b}\pi r_0^2). \tag{8}$$

For each BS $x\in\Pi_b$, a mark r_x is applied to represent the distance of its intended MU. The intended MU is a cell-interior user with $r_x \le c_0$, otherwise, it is a cell-edge user.

The interference at the typical MU is approximated as

$$\mathcal{I}_\mathrm{p} \approx \sum_{x\in\Pi_\mathrm{b}\setminus\{x_0\}} P_x G_x \ell_x^{-\alpha}, \tag{9}$$

where $P_x = \mathbf{1}(r_x\le c_0)+\eta\mathbf{1}(r_x>c_0)$. The indicator random variable $\mathbf{1}(\mathcal{A})$ equals 1 if condition $\mathcal{A}$ is satisfied, otherwise it equals 0. The indicator random variable denotes whether the interfering BS communicates with a cell-interior MU with normalized unit power or communicates with a cell-edge MU with normalized power $\eta\ge 1$. The approximation is given because the position of the cooperative SU is not the same as its serving BS when it performs the retransmission towards the cell-edge MU. The location of the relaying SU in the cell of $x\in\Pi_\mathrm{b}$ (the intended MU of x is at cell-edge) is denoted as $x_z = x+f(x)$, where $f(x)$ is the relative location of the selected SU from its serving BS x. Since almost surely we have $|f(x)|<\infty$, the distance between the selected SU and the typical MU can be approximated as the distance between its serving BS and the typical MU [25].

B. Success Probability of Cell-Interior Communication

Conditioned on the distance between BS x_0 and its typical cell-interior MU being r_0, the achievable rate of primary data transmission is expressed as

$$R_{\mathrm{in1}}(r_0) = (1-\beta)\log_2\Big(1+\frac{G_{x_0}r_0^{-\alpha}}{\mathcal{I}_{\mathrm{p}}}\Big), \tag{10}$$

where $(1-\beta)$ is the fraction of bandwidth kept by the primary system. Let T_0 denote the primary target rate, the success probability of original data transmission is obtained as

$$\begin{aligned} P_{\mathrm{in1}}(\tau_0, r_0) &= \mathbb{P}\big\{R_{\mathrm{in1}}(r_0) \geq T_0\big\} = \mathbb{P}\left\{G_{x_0} \geq \tau_0 r_0^{\alpha}\mathcal{I}_{\mathrm{p}}\right\} \\ &= \mathbb{E}\left[\exp\left(-\tau_0 r_0^{\alpha}\mathcal{I}_{\mathrm{p}}\right)\right] = \mathscr{L}_{\mathcal{I}_{\mathrm{p}}}(\tau_0 r_0^{\alpha}), \end{aligned} \tag{11}$$

where $\tau_0 = 2^{\frac{T_0}{1-\beta}} - 1$ and $\mathscr{L}_{\mathcal{I}_{\mathrm{p}}}(\cdot)$ represents the Laplace transform of the interference $\mathcal{I}_{\mathrm{p}}$. The exponential distribution of G_{x_0} is considered to obtain the expectation term in (11), which is taken over all possible locations and channel fadings of interferers in other cells. Here, both the spatial average and the time average over the interference are performed to obtain the average success probability. The locations of MUs are coupled by the locations of their serving BSs upon the *Poisson Tessellation* over the 2-D plane. Therefore, the communication distances and transmit powers of BSs towards their intended MUs in different cells are dependent. However, the dependence in different cells is weak as validated in [34]. For different cells, the distances between BSs and their intended MUs are assumed to be independent. The Laplace transform of $\mathcal{I}_{\mathrm{p}}$ can thus be derived as

$$\begin{aligned} \mathscr{L}_{\mathcal{I}_{\mathrm{p}}}(s) &= \mathbb{E}\Big[\exp\Big(-s\sum_{x\in\Pi_{\mathrm{b}}\setminus\{x_0\}} P_x G_x \ell_x^{-\alpha}\Big)\Big] \\ &\overset{(a)}{=} \mathbb{E}_{\Pi_{\mathrm{b}}}\Big\{\prod_{x\in\Pi_{\mathrm{b}}\setminus\{x_0\}} \mathbb{E}_{P,G}\Big[\exp\big(-sPG\ell_x^{-\alpha}\big)\Big]\Big\} \\ &\overset{(b)}{=} \exp\Big\{-2\pi\lambda_{\mathrm{b}}\mathbb{E}_{P,G}\Big[\int_{r_0}^{\infty}\big[1-\exp(-sP\ell^{-\alpha}G)\big]\,\ell\,\mathrm{d}\ell\Big]\Big\} \\ &\overset{(c)}{=} \exp\Big\{-2\pi\lambda_{\mathrm{b}}d_1\mathbb{E}_G\Big[\int_{r_0}^{\infty}\big[1-\exp(-s\ell^{-\alpha}G)\big]\,\ell\,\mathrm{d}\ell\Big]\Big\} \\ &\times \exp\Big\{-2\pi\lambda_{\mathrm{b}}d_2\mathbb{E}_G\Big[\int_{r_0}^{\infty}\big[1-\exp(-s\eta\ell^{-\alpha}G)\big]\,\ell\,\mathrm{d}\ell\Big]\Big\}, \end{aligned} \tag{12}$$

where $d_1 = 1-\exp(-\lambda_{\mathrm{b}}\pi c_0^2)$ and $d_2 = \exp(-\lambda_{\mathrm{b}}\pi c_0^2)$. Equality (a) is obtained due to the independence of channel fading and transmit power for each BS. Equality (b) is obtained according to the probability generating functional (PGFL) of PPP [33] and the integral is taken over (r_0,∞) as the interfering BSs are at least r_0 away from the typical MU. Taking the expectation of independent discrete random variable P, we obtain equality (c). By substituting $s = \tau_0 r_0^{\alpha}$ into (12) and calculating the integral over distance ℓ, we have

$$P_{\mathrm{in1}}(\tau_0, r_0) = \exp\left[-\omega(\tau_0)r_0^2\right], \tag{13}$$

where

$$\begin{aligned} \omega(t) = \pi\lambda_{\mathrm{b}}\Big\{&-1+\frac{d_1}{t+1}+\frac{d_2}{\eta t+1}+\Gamma(1-2/\alpha) \\ &\times\sum_{n=0}^{\infty}\frac{\Gamma(n+2)\,t^{n+1}}{\Gamma(n+2-2/\alpha)}\Big[\frac{d_1}{(t+1)^{n+2}}+\frac{d_2\eta^{n+1}}{(\eta t+1)^{n+2}}\Big]\Big\}. \end{aligned} \tag{14}$$

The Gamma function is $\Gamma(a) = \int_0^{\infty} t^{a-1}e^{-t}\,\mathrm{d}t$ and $\Gamma(n) = (n-1)!$ with $n = 1, 2, \ldots$ [35].

If the original transmission fails, the retransmission is performed by BS with achievable rate

$$R_{\mathrm{in2}}(r_0) = \frac{1-\beta}{2}\log_2\Big(1+\frac{2G_{x_0}r_0^{-\alpha}}{\mathcal{I}_{\mathrm{p}}}\Big), \tag{15}$$

where the pre-factor $1/2$ is applied due to the retransmission and the double SIR is used due to the MRC detection. The conditional success probability of this case is derived as

$$\begin{aligned} P_{\mathrm{in2}}(\tau_0, r_0) &= \mathbb{P}\big\{R_{\mathrm{in1}}(r_0) < T_0, R_{\mathrm{in2}}(r_0) \geq T_0/2\big\} \\ &= \exp\left[-\omega(\tau_0/2)r_0^2\right] - \exp\left[-\omega(\tau_0)r_0^2\right], \end{aligned} \tag{16}$$

where $\omega(\cdot)$ is given by (14).

C. Success Probability of Cell-Edge Communication

The communication between a BS and its cell-edge MU includes three cases: Case I, the MU correctly receives the primary data in the original phase; Case II, the original data transmission fails, there are no decoding SUs in the cooperation region, and the BS retransmits; Case III, the original data transmission fails, and a decoding SU is successfully selected to retransmit. Then, we analyze the three cases separately.

1) For Case I: Conditioned on the distance between BS x_0 and its typical cell-edge MU being r_0, the achievable rate of primary data transmission is expressed as

$$R_{\mathrm{ed}}(r_0) = (1-\beta)\log_2\Big(1+\frac{\eta G_{x_0}r_0^{-\alpha}}{\mathcal{I}_{\mathrm{p}}}\Big). \tag{17}$$

Similar to (13), the conditional success probability of original data transmission is derived as

$$P_{\mathrm{ed1}}(\tau_0, r_0) = \mathbb{P}\big\{R_{\mathrm{ed}}(r_0) \geq T_0\big\} = \exp\left[-\omega(\tau_0/\eta)r_0^2\right], \tag{18}$$

where $\omega(\cdot)$ is given in (14).

2) For Case II: The conditional success probability is

$$\begin{aligned} P_{\mathrm{ed2}}(\tau_0, r_0) = &\sum_{n=0}^{\infty}\Pr\left\{N=n\right\} \\ &\times\mathbb{P}\left\{\tau_0/2 \leq \gamma_{x_0} < \tau_0, \max\left\{\gamma_{x_0,z_i}\right\} < \tau_0\right\}, \end{aligned} \tag{19}$$

where the Poisson random variable N represents the number of SUs in the cooperation region. The probability is given as

$$\Pr\left\{N=n\right\} = \frac{(\lambda_{\mathrm{s}}\pi c_1^2)^n}{n!}\exp(-\lambda_{\mathrm{s}}\pi c_1^2). \tag{20}$$

The SIRs encountered at the typical MU and the ith SU in the cooperation region are given as

$$\gamma_{x_0} = \frac{\eta G_{x_0}r_0^{-\alpha}}{\mathcal{I}_{\mathrm{p}}} \quad \text{and} \quad \gamma_{x_0,z_i} = \frac{\eta G_{x_0,z_i}r_v^{-\alpha}}{\mathcal{I}_{\mathrm{p}_i}}, \tag{21}$$

where the distance between a BS and its cooperating SUs is set the same as $r_v = \zeta r_0$ $(0 < \zeta < 1)$. The interference at the ith SU is denoted as $\mathcal{I}_{\mathrm{p}_i}$. When $N = 0$, the success probability of (19) is reduced as $\tilde{P}_{\mathrm{ed2}}(\tau_0, r_0) = \mathbb{P}\{\tau_0/2 \le \gamma_{x_0} < \tau_0\}$ and it is derived as follows similarly to (16),

$$\tilde{P}_{\mathrm{ed2}}(\tau_0, r_0) = \exp\left[-\omega(\tau_0/(2\eta))r_0^2\right] - \exp\left[-\omega(\tau_0/\eta)r_0^2\right], \tag{22}$$

where $\omega(\cdot)$ is given by (14).

When the original transmission fails, the success probability of BS doing the retransmission is obtained as (please see Appendix I for the derivation)

$$P_{\mathrm{ed2}}(\tau_0, r_0) = \exp(-\lambda_{\mathrm{s}}\pi c_1^2)\tilde{P}_{\mathrm{ed2}}(\tau_0, r_0) + \sum_{n=1}^{\infty} \frac{(\lambda_{\mathrm{s}}\pi c_1^2)^n}{n!} \exp(-\lambda_{\mathrm{s}}\pi c_1^2) f_1(\tau_0, r_0, n), \tag{23}$$

where

$$f_1(\tau_0, r_0, n) = \sum_{k=0}^{n} (-1)^k \binom{n}{k} \Big\{ \exp\left[-g(\tau_0, r_0^\alpha/2, k)\right] - \exp\left[-g(\tau_0, r_0^\alpha, k)\right] \Big\}, \tag{24}$$

with

$$g(\tau_0, s, k) = 2\pi\lambda_{\mathrm{b}} \int_{r_0}^{\infty} \left[1 - \frac{d_1}{(1 + \frac{\tau_0 s}{\eta}\ell^{-\alpha})(1 + \frac{\tau_0 r_v^\alpha}{\eta}\ell^{-\alpha})^k} - \frac{d_2}{(1 + \tau_0 s\ell^{-\alpha})(1 + \tau_0 r_v^\alpha \ell^{-\alpha})^k} \right] \ell \, \mathrm{d}\ell. \tag{25}$$

Since only one-dimensional integral is included in (25), it can be calculated efficiently.

3) For Case III: In this case, the original data transmission between BS and its intended cell-edge MU fails, but at least one SU in the cooperation region correctly receives the data. Each decoding SU can estimate its channel state towards the cell-edge MU through measuring the strength of NACK frame. According to the channel quality, each SU can initiate a back-off timer [17] or transmit a burst sequence [31] to compete for the channel access. The decoding SU with the best channel state towards the cell-edge MU can be selected to retransmit. The conditional success probability is given as

$$P_{\mathrm{ed3}}(\tau_0, r_0) = \sum_{n=1}^{\infty} \Pr\{N = n\} \times \sum_{k=1}^{n} \mathbb{P}\Big\{\gamma_{x_0} < \tau_0, |\Phi_{x_0}| = k, \gamma_{x_0} + \max_{i \in \Phi_{x_0}} \{\gamma_{z_i}\} \ge \tau_0\Big\}, \tag{26}$$

where γ_{x_0} is the SIR between BS x_0 and its cell-edge MU as given in (21). The probability of there being $n \neq 0$ SUs in the cooperation region is $\Pr\{N = n\}$ given by (20). The inequality $\gamma_{x_0} < \tau_0$ represents that the original transmission between BS and its cell-edge MU fails. The term $|\Phi_{x_0}| = k$ represents that the cardinality of the decoding set is k, where Φ_{x_0} is the decoding set of SUs in the cooperation region. The term $\gamma_{x_0} + \max_{i \in \Phi_{x_0}}\{\gamma_{z_i}\} \ge \tau_0$ represents that the MRC detection is successful at the cell-edge MU, when the retransmission is performed by the best decoding SU. The SIR between a decoding SU z_i, $i \in \Phi_{x_0}$ and the typical MU is $\gamma_{z_i} = \frac{\eta G_{z_i} \tilde{r}_v^{-\alpha}}{\mathcal{I}_{\mathrm{p}}}$ with $\tilde{r}_v = r_0 - r_v = (1 - \zeta)r_0$ denoting the distance between the cooperation region center and the cell-edge MU. Since the relaying SUs lie in the cooperation region with small radius, the distance between each decoding SU and the cell-edge MU is set the same as $\tilde{r}_v$. As derived in Appendix II, the conditional success probability is given by

$$P_{\mathrm{ed3}}(\tau_0, r_0) = \sum_{n=1}^{\infty} \frac{(\lambda_{\mathrm{s}}\pi c_1^2)^n}{n!} \exp(-\lambda_{\mathrm{s}}\pi c_1^2) f_2(\tau_0, r_0, n), \tag{27}$$

where

$$f_2(\tau_0, r_0, n) = \sum_{k=1}^{n} \binom{n}{k} \sum_{m=0}^{n-k} \binom{n-k}{m} (-1)^m \times \Bigg\{ \exp\left[-g(\tau_0, 0, m+k)\right] - \Big[\sum_{t=0}^{k} \binom{k}{t} \frac{(-1)^t r_0^\alpha}{t\tilde{r}_v^\alpha - r_0^\alpha} + 1\Big] \times \exp\left[-g(\tau_0, r_0^\alpha, m+k)\right] + \sum_{t=0}^{k} \binom{k}{t} \frac{(-1)^t r_0^\alpha}{t\tilde{r}_v^\alpha - r_0^\alpha} \times \exp\left[-g(\tau_0, t\tilde{r}_v^\alpha, m+k)\right] \Bigg\}, \tag{28}$$

with the function $g(\cdot, \cdot, \cdot)$ given by (25).

D. Average Throughput of Primary System

If there is no spectrum sharing, the traditional truncated ARQ scheme with one-time retransmission is applied in the stand-alone cellular network. By averaging over the random variable R, we can obtain the average throughput of cellular network downlink as

$$V_{\mathrm{d}} = \underbrace{\int_0^{c_0} T_0\left[P_{\mathrm{in1}}(\hat{\tau}_0, r_0) + (1/2)P_{\mathrm{in2}}(\hat{\tau}_0, r_0)\right] f_R(r_0)\, \mathrm{d}r_0}_{V_{\mathrm{din}}(\hat{\tau}_0)} + \underbrace{\int_{c_0}^{\infty} T_0\left[P_{\mathrm{ed1}}(\hat{\tau}_0, r_0) + (1/2)\tilde{P}_{\mathrm{ed2}}(\hat{\tau}_0, r_0)\right] f_R(r_0)\, \mathrm{d}r_0}_{V_{\mathrm{ded}}(\hat{\tau}_0)}, \tag{29}$$

where $\hat{\tau}_0 = 2^{T_0} - 1$. The conditional success probabilities of original data transmission and retransmission for the cell-interior MU and cell-edge MU are given as $P_{\mathrm{in1}}(\hat{\tau}_0, r_0)$, $P_{\mathrm{in2}}(\hat{\tau}_0, r_0)$, $P_{\mathrm{ed1}}(\hat{\tau}_0, r_0)$, and $\tilde{P}_{\mathrm{ed2}}(\hat{\tau}_0, r_0)$, which can be obtained by replacing τ_0 in (13), (16), (18), and (22) with $\hat{\tau}_0$, respectively. By substituting the related expressions into (29), the average throughput of cell-interior communication is

$$V_{\mathrm{din}}(\hat{\tau}_0) = \frac{T_0\lambda_{\mathrm{b}}\pi}{2[\lambda_{\mathrm{b}}\pi + \omega(\hat{\tau}_0)]} \left\{1 - \exp\left[-(\lambda_{\mathrm{b}}\pi + \omega(\hat{\tau}_0))c_0^2\right]\right\} + \frac{T_0\lambda_{\mathrm{b}}\pi}{2[\lambda_{\mathrm{b}}\pi + \omega(\hat{\tau}_0/2)]} \left\{1 - \exp\left[-(\lambda_{\mathrm{b}}\pi + \omega(\hat{\tau}_0/2))c_0^2\right]\right\}. \tag{30}$$

Similarly, the average throughput of cell-edge link is given as

$$V_{\mathrm{ded}}(\hat{\tau}_0) = \frac{T_0\lambda_{\mathrm{b}}\pi}{2[\lambda_{\mathrm{b}}\pi + \omega(\hat{\tau}_0/\eta)]} \exp\left\{-\left[\lambda_{\mathrm{b}}\pi + \omega(\hat{\tau}_0/\eta)\right] c_0^2\right\} + \frac{T_0\lambda_{\mathrm{b}}\pi}{2[\lambda_{\mathrm{b}}\pi + \omega(\hat{\tau}_0/(2\eta))]} \exp\left\{-\left[\lambda_{\mathrm{b}}\pi + \omega(\hat{\tau}_0/(2\eta))\right] c_0^2\right\}. \tag{31}$$

$$V_{\rm c}(\lambda_{\rm s},\beta)=\underbrace{\int_0^{c_0} T_0\left[P_{\rm in1}(\tau_0,r_0)+(1/2)P_{\rm in2}(\tau_0,r_0)\right]f_{\rm R}(r_0)\,{\rm d}r_0}_{V_{\rm cin}(\tau_0)}$$
$$+\underbrace{\int_{c_0}^{\infty} T_0\left[P_{\rm ed1}(\tau_0,r_0)+(1/2)P_{\rm ed2}(\tau_0,r_0)+(1/2)P_{\rm ed3}(\tau_0,r_0)\right]f_{\rm R}(r_0)\,{\rm d}r_0}_{V_{\rm ced}(\tau_0)}. \quad (32)$$

$$\begin{aligned}V_{\rm ced}(\tau_0)=&\frac{T_0\lambda_{\rm b}\pi\left[2-\exp(-\lambda_{\rm s}\pi c_1^2)\right]}{2\left[\lambda_{\rm b}\pi+\omega(\tau_0/\eta)\right]}\exp\left\{-\left[\lambda_{\rm b}\pi+\omega\left(\tau_0/\eta\right)\right]c_0^2\right\}\\&+\frac{T_0\lambda_{\rm b}\pi\exp(-\lambda_{\rm s}\pi c_1^2)}{2\left[\lambda_{\rm b}\pi+\omega(\tau_0/(2\eta))\right]}\exp\left\{-\left[\lambda_{\rm b}\pi+\omega\left(\tau_0/(2\eta)\right)\right]c_0^2\right\}\\&+\frac{T_0\lambda_{\rm b}\pi}{\exp(\lambda_{\rm s}\pi c_1^2)}\sum_{n=1}^{\infty}\frac{(\lambda_{\rm s}\pi c_1^2)^n}{n!}\int_{c_0}^{\infty} r_0\left[f_1(\tau_0,r_0,n)+f_2(\tau_0,r_0,n)\right]\exp(-\lambda_{\rm b}\pi r_0^2)\,{\rm d}r_0. \quad (33)\end{aligned}$$

The average throughput of primary system with cooperative spectrum sharing is obtained as $V_{\rm c}(\lambda_{\rm s},\beta)$ on the top of next page. In (32), $V_{\rm cin}(\tau_0)=V_{\rm din}(\tau_0)$ is obtained by replacing $\hat{\tau}_0$ with τ_0 in (30). The other integral in (32) is derived by (33), where $f_1(\tau_0,r_0,n)$ and $f_2(\tau_0,r_0,n)$ are given by (24) and (28), respectively. The closed form expression of the integral in (33) is not available, but it can be numerically calculated. Without losing accuracy, the last term of (33) can be calculated with limited number of n.

V. Solution to the Optimization Problem

In this section, we will find the optimal $\lambda_{\rm s}$ and β that can maximize the secondary transmission capacity (1) while satisfying the constraints (2) and (3). The transmission capacity of secondary system is a monotonically increasing function of the SU density $\lambda_{\rm s}$. Therefore, the higher the SU density, the higher the transmission capacity. However, the outage performance of secondary system gets worse with higher SU density as more interference is introduced. The maximum SU density that can satisfy the outage constraint (2) is obtained via $P_{\rm out}^{\rm s}(\lambda_{\rm s},\beta)=\epsilon$. Then, we can obtain one critical point of the SU density as

$$\lambda_{\rm s1}(\beta)=-\frac{\ln(1-\epsilon)}{\xi\pi d^2\tau_1^{2/\alpha}}\frac{\sin(2\pi/\alpha)}{2\pi/\alpha}. \quad (34)$$

This critical density is a function of the bandwidth allocation factor β included in $\tau_1=2^{T_1/\beta}-1$. We can see that $\lambda_{\rm s1}(\beta)$ is a monotonically increasing function of the bandwidth allocation factor β. The more bandwidth allocated to the secondary system, the more concurrent secondary links can be allowed without violating the outage probability constraint in the optimization problem. We note that the outage constraint is guaranteed only when $\lambda_{\rm s}\le\lambda_{\rm s1}(\beta)$.

The higher the SU density, the more SUs lying in the cooperation region and the higher the average throughput of primary downlink. Through setting $V_{\rm c}(\lambda_{\rm s},\beta)=(1+\rho)V_{\rm d}$ in the constraint (3), we can find another critical point $\lambda_{\rm s2}(\beta)$, which is also a function of β. For a given β, the throughput improvement requirement of primary system can be satisfied only when $\lambda_{\rm s}\ge\lambda_{\rm s2}(\beta)$.

Therefore, for a given $\beta\in(0,1)$, both constraints (2) and (3) can be satisfied with $\lambda_{\rm s2}(\beta)\le\lambda_{\rm s}\le\lambda_{\rm s1}(\beta)$. To maximize the transmission capacity of secondary system, we need to search for the values of β and its corresponding $\lambda_{\rm s1}(\beta)$ and $\lambda_{\rm s2}(\beta)$. A given β belongs to the potential allocation set $\mathcal{S}$ if we have $\lambda_{\rm s2}(\beta)\le\lambda_{\rm s1}(\beta)$, i.e., $\mathcal{S}=\{\beta\in(0,1):\lambda_{\rm s2}(\beta)\le\lambda_{\rm s1}(\beta)\}$. The optimal bandwidth allocation factor is denoted as β^* and obtained as $\beta^*=\arg\max_{\beta\in\mathcal{S}}\lambda_{\rm s1}(\beta)$. The optimal SU density is obtained as $\lambda_{\rm s1}(\beta^*)$ and the transmission capacity of secondary system can thus be derived as $C_{\rm s}^{\epsilon}=\xi\lambda_{\rm s1}(\beta^*)(1-\epsilon)T_1$. Using this solution, the throughput of primary system can be improved by at least the ratio ρ. However, if $\mathcal{S}=\emptyset$, the two constraints of the optimization problem cannot be satisfied simultaneously and the cellular network will utilize the whole spectrum band for its own data transmission without secondary access.

To numerically search the optimal bandwidth allocation factor and the maximum SU density, we use the following approach. For each value of $\beta\in(0,1)$, we calculate $\lambda_{\rm s1}(\beta)$ according to (34) and $\hat{\rho}=\left[V_{\rm c}(\lambda_{\rm s1}(\beta),\beta)-V_{\rm d}\right]/V_{\rm d}$. If $\hat{\rho}<\rho$ occurs, $\lambda_{\rm s2}(\beta)$ is larger than $\lambda_{\rm s1}(\beta)$, so this bandwidth allocation factor is not a potential point, i.e, $\beta\notin\mathcal{S}$. If $\hat{\rho}\ge\rho$ occurs, $\lambda_{\rm s2}(\beta)$ is no larger than $\lambda_{\rm s1}(\beta)$, so this bandwidth allocation factor is potential, i.e., $\beta\in\mathcal{S}$. Over the whole potential allocation set $\mathcal{S}$, we can find the one that brings the largest SU density.

VI. Numerical and Simulation Results

In this section, we show the impacts of system parameters to the primary performance and verify our theoretical analysis of Section IV. The transmission capacities of secondary system with different system settings are plotted by solving the optimization problem of Section III. The simulation results are obtained by averaging over the topology iterations for 10^5 times, and the overlaid network is modeled as a circular area over the 2-D plane with radius $\sqrt{10}\times10^2$ m. Similarly to reference [27], the optimal power ratio is set as $\eta^*=\arg\max_{\eta\in[1,20]}V_{\rm d}$.

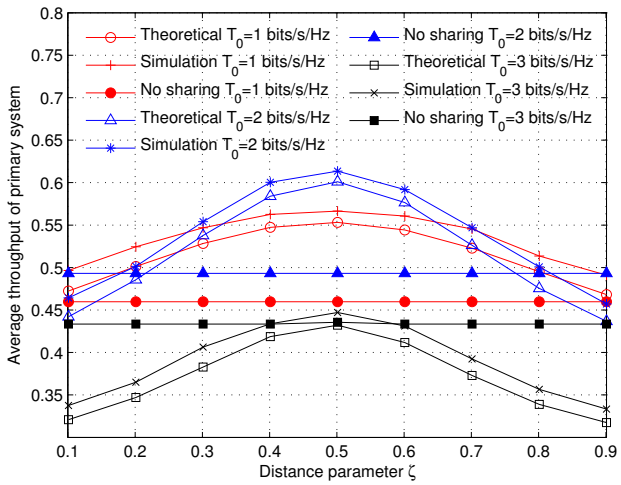

Fig. 4. Average throughput of the primary system w.r.t. the relative distance ζ. The system settings are $\alpha = 3$, $c_0 = 9$ m, $c_1 = 1$ m, $\lambda_b = 10^{-3}$, $\lambda_m = 10^{-2}$, and $\lambda_s = 0.9$. The bandwidth allocation $\beta = 0.2$ is used for the cooperative spectrum sharing, while it is zero for the stand-alone cellular network without spectrum sharing. The theoretical results are obtained from (32).

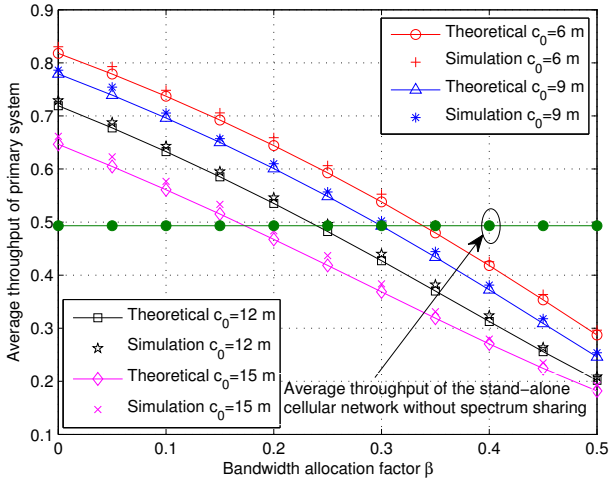

Fig. 5. Average throughput of the primary system w.r.t. the bandwidth allocation factor β. The system settings are $\alpha = 3$, $c_1 = 1$ m, $\zeta = 0.501$, $T_0 = 2$ bits/s/Hz, $\lambda_b = 10^{-3}$, $\lambda_m = 10^{-2}$, and $\lambda_s = 0.9$. The theoretical results are obtained from (32).

A. Average Throughput of Primary System

Fig. 4 shows the average throughput of cellular network downlink with respect to the distance factor ζ for different values of primary target rate T_0. In the cooperative spectrum sharing, the best performance of primary system can be achieved when $\zeta = 0.5$. The cooperation region should be located in the middle between each BS and its intended cell-edge MU. When ζ is small, the cooperation region is close to the BS and it is more likely to select one decoding SU to help the primary data transmission. As the distance towards the cell-edge MU is far, the robustness of cooperative communicaiton is weak. On the other hand, when ζ is large, the cooperation region is far from the BS and the decoding set is more likely empty. As a result, the opportunity of cooperation is small. Therefore, the primary performance is worse in both the small and large regions of ζ. The throughput is defined as the product of target rate T_0 and success probability, which gets worse with the increase of T_0. With the variation of T_0, the primary throughput is a trade-off between target rate and success probability. Since a fraction of spectrum is released for the secondary data transmission, the throughput of primary system may be worse than that without spectrum sharing.

Fig. 5 shows the primary average throughput with respect to the bandwidth allocation factor β for different sizes of cell-interior area. The more bandwidth allocated to the secondary system, the less throughput is obtained for the primary system, as it becomes more difficult to support the primary target rate with the remaining narrower bandwidth $1 - \beta$. When $\beta = 0$, no spectrum is allocated to the secondary system, but the primary transmission is assisted by SUs, so the throughput greatly outperforms the stand-alone cellular network without spectrum sharing. The average throughput of primary downlink improves with the decrease of the division radius c_0. The smaller the cell-interior area, the larger the cell-edge area,

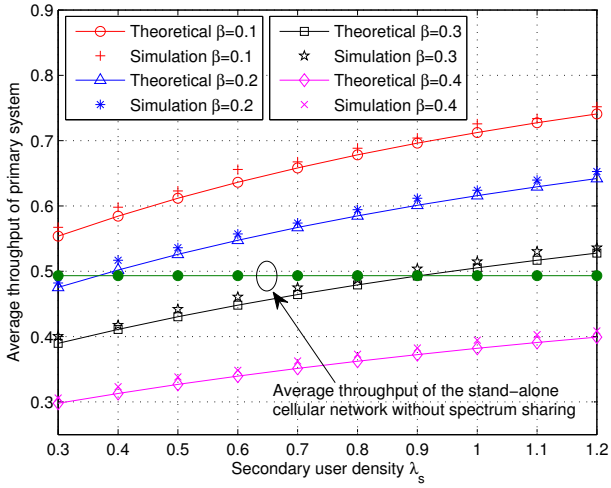

Fig. 6. Average throughput of the primary system w.r.t. the SU density λ_s. The system settings are $\alpha = 3$, $c_0 = 9$ m, $c_1 = 1$ m, $\zeta = 0.501$, $T_0 = 2$ bits/s/Hz, $\lambda_b = 10^{-3}$, and $\lambda_m = 10^{-2}$. The theoretical results are obtained from (32).

and hence more benefits can be brought by the cooperation from SUs. The numerical results of Section IV are tight to the simulation results.

Fig. 6 shows the impact of SU density λ_s to the primary performance with different values of bandwidth allocation factor β. The region division radius of each cell is set as $c_0 = 9$ m, while the radius of the cooperation region is set as $c_1 = 1$. The average throughput of the primary downlink deteriorates with the decrease of the SU density λ_s. This is because the smaller the SU density λ_s, the less average number of SUs residing in the cooperation region for the possible retransmission of primary data. It also shows that the larger time allocation factor β results in the smaller primary throughput. Our theoretical analysis can well match

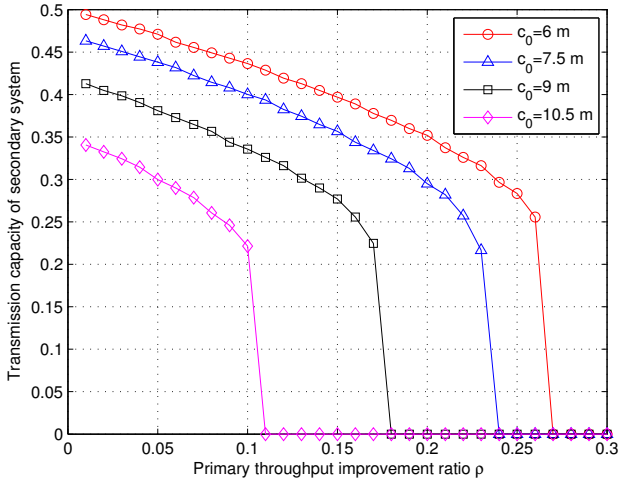

Fig. 7. Transmission capacity of secondary system w.r.t. the primary throughput improvement ratio ρ for different c_0. The system settings are $\alpha = 3$, $c_1 = 1$ m, $\zeta = 0.501$, $T_0 = 2$ bits/s/Hz, $T_1 = 1$ bits/s/Hz, $\epsilon = 0.1$, $\xi = 0.2$, $d = 0.1$, and $\lambda_b = 10^{-3}$.

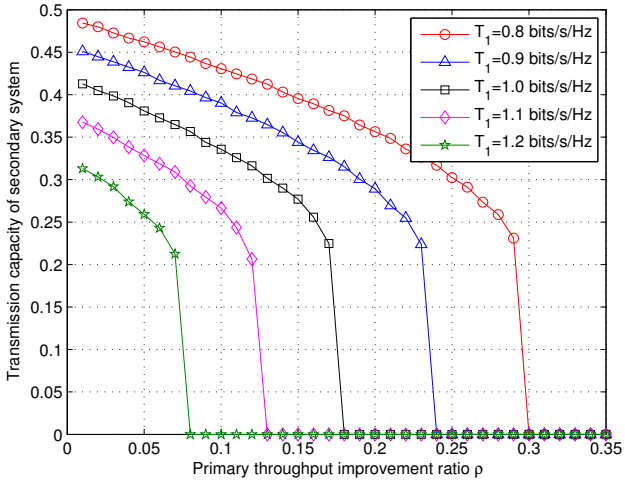

Fig. 8. Transmission capacity of secondary system w.r.t. the primary throughput improvement ratio ρ for different T_1. The system settings are $\alpha = 3$, $c_0 = 9$ m, $c_1 = 1$ m, $\zeta = 0.501$, $T_0 = 2$ bits/s/Hz, $\epsilon = 0.1$, $\xi = 0.2$, $d = 0.1$, and $\lambda_b = 10^{-3}$.

the simulation results.

B. Transmission Capacity of Secondary System

Fig. 7 shows the secondary transmission capacity against the primary throughput improvement ratio ρ with different cell division radius c_0. The secondary transmission capacity gets worse with the increase of ρ and it becomes zero when ρ is larger than a critical point, which is an upper bound of the primary throughput improvement ratio. In other words, the throughput improvement ratio larger than this critical point cannot be achieved by the cooperative spectrum sharing scheme. The secondary transmission capacity deteriorates with the increase of radius c_0. The cell-edge area is small when c_0 is large, so the potential improvement of primary performance is small due to the small opportunity of cooperative data transmission. Therefore, the secondary performance gets worse as more resource is reserved to meet the primary QoS requirement.

Fig. 8 shows the secondary transmission capacity versus the primary throughput improvement ratio ρ for different secondary target rate T_1. Similarly, there is an upper bound of the parameter ρ, above which the primary requirement can not be satisfied and the cooperative spectrum sharing is inactive. The secondary transmission capacity gets smaller with the increase of target rate T_1. This phenomenon is attributable to a trade-off between the maximum allowable SU density and the transmission rate. The outage probability of secondary data transmission gets worse with the increase of T_1 as shown by (6). Therefore, the allowable maximum SU density λ_s becomes smaller to satisfy the constraint of target outage probability ϵ as can be seen from (34). Since the negative effect of SU density reduction dominates over the positive effect of transmission rate increase, the secondary transmission capacity gets worse.

Fig. 9 shows the secondary transmission capacity with respect to the secondary target outage probability ϵ for different

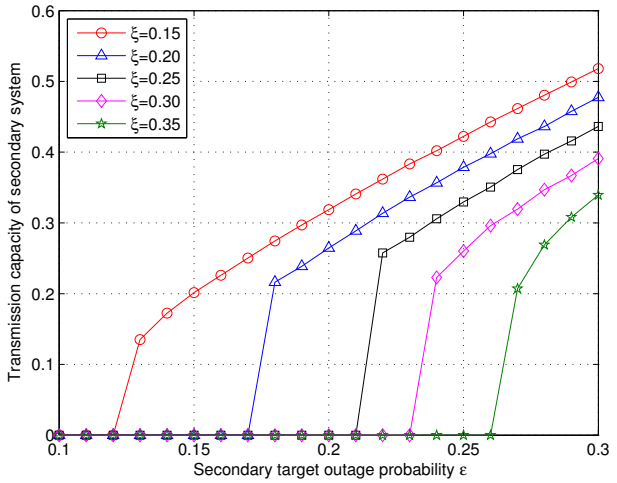

Fig. 9. Transmission capacity of secondary system w.r.t. the secondary target outage probability ϵ for different ξ. The system settings are $\alpha = 3$, $c_0 = 9$ m, $c_1 = 1$ m, $\zeta = 0.501$, $T_0 = 2$ bits/s/Hz, $T_1 = 1$ bits/s/Hz, $d = 0.15$, $\rho = 0.1$, and $\lambda_b = 10^{-3}$.

Aloha MAP ξ. With the primary throughput improvement ratio fixed, there exists a critical value of ϵ, below which the primary performance improvement requirement cannot be guaranteed and the cooperative spectrum sharing is not valid. Above this critical point, the secondary transmission capacity gets larger with the increase of target outage probability ϵ. The larger the target outage probability, the larger the maximum allowable SU density as shown by (34). Although the success probability of secondary data transmission becomes worse with the increase of ϵ, the benefits brought by the SU density increase can beat against the degradation of success probability. As a compromise, the secondary transmission capacity gets better. With the increase of ξ, the maximum allowable SU density gets smaller and less cooperation is performed for the primary

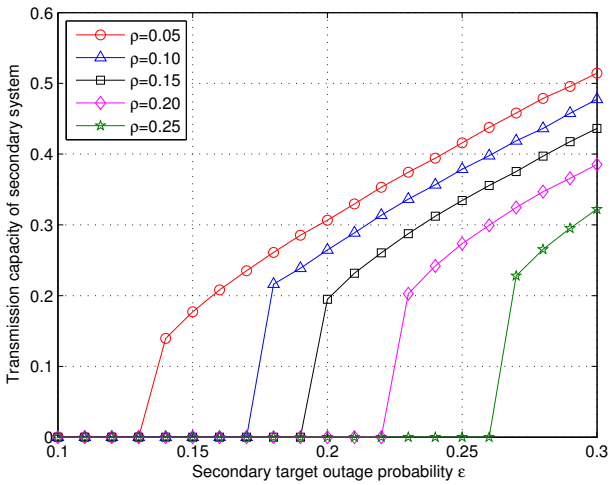

Fig. 10. Transmission capacity of secondary system w.r.t. the secondary target outage probability ϵ for different ρ. The system settings are $\alpha = 3$, $c_0 = 9$ m, $c_1 = 1$ m, $\zeta = 0.501$, $T_0 = 2$ bits/s/Hz, $T_1 = 1$ bits/s/Hz, $d = 0.15$, $\xi = 0.2$, and $\lambda_{\rm b} = 10^{-3}$.

cell-edge communication. As a result, less resource is allocated for the secondary data transmission, and hence the secondary transmission capacity gets worse.

Fig. 10 shows the secondary transmission capacity against the secondary target outage probability ϵ with different primary throughput improvement ratio ρ. Similarly, there is a critical point of ϵ, bellow which the cooperative spectrum sharing cannot be performed, as the primary performance constraint is violated. The secondary transmission capacity deteriorates with the increase of ρ, because it is more difficult to meet the primary performance requirement and more resource is kept for the primary data transmission. In this situation, less resource is available for the secondary data transmission and hence the secondary transmission capacity gets smaller.

VII. Conclusion

In this paper, we design a cooperative spectrum sharing scheme between cellular network downlink and ad-hoc network. The secondary users can actively help the primary cell-edge communication to improve the primary performance by a predefined ratio. As a reward, a fraction of disjoint bandwidth can be released for the secondary data transmission. The transmission capacity of secondary system and the average throughput of primary downlink are analyzed using the stochastic geometry theory. The optimization problem is formulated to maximize the secondary transmission capacity under the QoS constraints of secondary outage probability and primary throughput improvement. The optimal secondary user density and bandwidth allocation are numerically calculated. Performance results are provided to demonstrate that the primary performance can be conservatively improved and the secondary transmission can be well accommodated.

Appendix I: Derivation of (23)

We assume that the distance between an interferer and each SU in the cooperation region is the same as the distance between this interferer and the typical cell-edge MU. The pathloss from an interferer to the cooperative SUs and to the typical MU is the same, while the channel fading is independent. The success probability in (19) is derived as

$$\begin{aligned}
&\mathbb{P}\Big\{\frac{\tau_0}{2} \le \gamma_{x_0} < \tau_0, \max_{i=1\to n}\{\gamma_{x_0,z_i}\} < \tau_0\Big\} \\
&= \mathbb{P}\left\{\frac{\tau_0}{2} \le \frac{\eta G_{x_0} r_0^{-\alpha}}{\mathcal{I}_{\rm p}} < \tau_0, \max\left\{\frac{\eta G_{x_0,z_i} r_v^{-\alpha}}{\mathcal{I}_{{\rm p}_i}}\right\} < \tau_0\right\} \\
&= \mathbb{E}_{\Pi_{\rm b},P}\Big\{\underbrace{\mathbb{E}_G\Big[\exp\big(-\frac{\tau_0 r_0^\alpha}{2\eta}\mathcal{I}_{\rm p}\big) - \exp\big(-\frac{\tau_0 r_0^\alpha}{\eta}\mathcal{I}_{\rm p}\big)\Big]}_{\mathcal{A}_1} \\
&\qquad \times \underbrace{\prod_{i=1}^{n}\mathbb{E}_G\Big[1-\exp\big(-\frac{\tau_0 r_v^\alpha}{\eta}\mathcal{I}_{{\rm p}_i}\big)\Big]}_{\mathcal{A}_2}\Big\}, \qquad (35)
\end{aligned}$$

where the inner expectations are taken over the independent channel fading from each interferer to the cell-edge MU and each cooperative SU. The outside expectation of (35) is taken over the point process and the transmit power of interferers. The expectation over the independent channel fading between interferers and the typical cell-edge MU, i.e., $\mathcal{A}_1$ of (35), is derived as

$$\mathcal{A}_1 = \prod_{x\in\Pi_{\rm b}\setminus\{x_0\}} \frac{1}{1+\frac{\tau_0 r_0^\alpha}{2\eta}P_x\ell_x^{-\alpha}} - \prod_{x\in\Pi_{\rm b}\setminus\{x_0\}} \frac{1}{1+\frac{\tau_0 r_0^\alpha}{\eta}P_x\ell_x^{-\alpha}} \qquad (36)$$

where this result is obtained by substituting the interference $\mathcal{I}_{\rm p}$ (9) and taking the expectation over the independent channel fading. Similarly, the expectation over the channel fading between interferers and SUs in the cooperation region, i.e., $\mathcal{A}_2$ of (35), is derived as

$$\mathcal{A}_2 = \left\{1 - \prod_{x\in\Pi_{\rm b}\setminus\{x_0\}} \frac{1}{1+\frac{\tau_0 r_v^\alpha}{\eta}P_x\ell_x^{-\alpha}}\right\}^n. \qquad (37)$$

Substitute (36) and (37) into (35), we can get the result as

$$\begin{aligned}
&\mathbb{P}\Big\{\frac{\tau_0}{2} \le \gamma_{x_0} < \tau_0, \max_{i=1\to n}\{\gamma_{x_0,z_i}\} < \tau_0\Big\} = \sum_{k=0}^{n}(-1)^k\binom{n}{k} \\
&\Big\{\underbrace{\mathbb{E}_{\Pi_{\rm b},P}\Big[\prod_{x\in\Pi_{\rm b}\setminus\{x_0\}} \frac{1}{\big(1+\frac{\tau_0 r_0^\alpha}{2\eta}P_x\ell_x^{-\alpha}\big)\big(1+\frac{\tau_0 r_v^\alpha}{\eta}P_x\ell_x^{-\alpha}\big)^k}\Big]}_{\mathcal{B}_1} \\
&\underbrace{-\,\mathbb{E}_{\Pi_{\rm b},P}\Big[\prod_{x\in\Pi_{\rm b}\setminus\{x_0\}} \frac{1}{\big(1+\frac{\tau_0 r_0^\alpha}{\eta}P_x\ell_x^{-\alpha}\big)\big(1+\frac{\tau_0 r_v^\alpha}{\eta}P_x\ell_x^{-\alpha}\big)^k}\Big]}_{\mathcal{B}_2}\Big\} \qquad (38)
\end{aligned}$$

where the binomial expansion of $\mathcal{A}_2$ is utilized. Then, applying the PGFL of PPP and taking the expectation over the BS transmit power, we can get the result of $\mathcal{B}_1$ of (38) as

$$\begin{aligned}
\mathcal{B}_1 = \exp\Big\{-2\pi\lambda_{\rm b}\int_{r_0}^{\infty}\Big[1 - \frac{d_1}{\big(1+\frac{\tau_0 r_0^\alpha}{2\eta}\ell^{-\alpha}\big)\big(1+\frac{\tau_0 r_v^\alpha}{\eta}\ell^{-\alpha}\big)^k} \\
- \frac{d_2}{\big(1+\frac{\tau_0 r_0^\alpha}{2}\ell^{-\alpha}\big)\big(1+\tau_0 r_v^\alpha\ell^{-\alpha}\big)^k}\Big]\ell\,{\rm d}\ell\Big\}, \qquad (39)
\end{aligned}$$

where the integral plus the pre-factor is denoted as a function $g\big(\tau_0, r_0^\alpha/2, k\big)$. Similarly, another expectation of (38) can be directly obtained as

$$\mathcal{B}_2 = \exp\big[-g\big(\tau_0, r_0^\alpha, k\big)\big]. \tag{40}$$

Then, jointly considering $\Pr\{N=n\}$ in (20) and the probability of (38), the success probability of Case II can thus be derived as (23).

Appendix II: Derivation of (27)

The probability of (26) is given as follows and it is further divided into two parts.

$$\begin{aligned}&\mathbb{P}\Big\{\gamma_{x_0} < \tau_0, |\Phi_{x_0}| = k, \gamma_{x_0} + \max_{i\in\Phi_{x_0}}\{\gamma_{z_i}\} \geq \tau_0\Big\}\\ &= \underbrace{\mathbb{P}\left\{\gamma_{x_0} < \tau_0, |\Phi_{x_0}| = k\right\}}_{\mathcal{C}_1}\\ &- \underbrace{\mathbb{P}\big\{\gamma_{x_0} < \tau_0, |\Phi_{x_0}| = k, \gamma_{x_0} + \max_{i\in\Phi_{x_0}}\{\gamma_{z_i}\} < \tau_0\big\}}_{\mathcal{C}_2}. \end{aligned}\tag{41}$$

Conditioned on the PPP Π_b and the transmit power P of interferers, the probability of a cooperating SU z_i correctly receiving the primary data is given as

$$\mathbb{P}\left\{\gamma_{x_0,z_i} \geq \tau_0 \big| \Pi_\mathrm{b}, P\right\} = \prod_{x\in\Pi_\mathrm{b}\setminus\{x_0\}} \frac{1}{1+\frac{\tau_0 r_v^\alpha}{\eta} P_x \ell_x^{-\alpha}}. \tag{42}$$

Then, the conditional probability of the cardinality of decoding set being k is derived as

$$\begin{aligned}&\mathbb{P}\left\{|\Phi_{x_0}| = k \big| \Pi_\mathrm{b}, P\right\} = \binom{n}{k}\Big[\mathbb{P}\left\{\gamma_{x_0,z_i} \geq \tau_0 \big| \Pi_\mathrm{b}, P\right\}\Big]^k\\ &\times \Big[1 - \mathbb{P}\left\{\gamma_{x_0,z_i} \geq \tau_0 \big| \Pi_\mathrm{b}, P\right\}\Big]^{n-k} = \binom{n}{k}\sum_{m=0}^{n-k}\binom{n-k}{m}\\ &\times (-1)^m \prod_{x\in\Pi_\mathrm{b}\setminus\{x_0\}} \frac{1}{\big(1+\frac{\tau_0 r_v^\alpha}{\eta} P_x \ell_x^{-\alpha}\big)^{m+k}}, \end{aligned}\tag{43}$$

where the binomial expansion is considered. The distance between an interferer and each SU in the cooperation region is set the same as the distance between this interferer and the typical cell-edge MU. Jointly considering the events that the original transmission fails and the decoding set has k SUs, taking expectation over the discrete random variable P and applying the PGFL of PPP, the first probability of (41) is derived as

$$\begin{aligned}\mathcal{C}_1 = \binom{n}{k}\sum_{m=0}^{n-k}\binom{n-k}{m}(-1)^m\Big\{&\exp\big[-g(\tau_0, 0, m+k)\big]\\ &- \exp\big[-g(\tau_0, r_0^\alpha, m+k)\big]\Big\}, \end{aligned}\tag{44}$$

where the function $g(\cdot,\cdot,\cdot)$ is given in (25).

Conditioned on the PPP Π_b and transmit power P of interferers, we can derive the following probability when there are k SUs in the decoding set Φ_{x_0}.

$$\begin{aligned}&\mathbb{P}\Big\{\gamma_{x_0} < \tau_0, \gamma_{x_0} + \max_{i\in\Phi_{x_0}}\{\gamma_{z_i}\} < \tau_0 \big| |\Phi_{x_0}| = k, \Pi_\mathrm{b}, P\Big\}\\ &= \mathbb{E}_G\Big\{\int_0^{\frac{\tau_0 r_0^\alpha}{\eta}\mathcal{I}_\mathrm{p}} \Big\{1 - \exp\Big[-\frac{(\tau_0-\gamma_{x_0})\tilde{r}_v^\alpha}{\eta}\mathcal{I}_\mathrm{p}\Big]\Big\}^k\\ &\qquad\times \exp(-G_{x_0})\,\mathrm{d}G_{x_0}\Big\}\\ &= \sum_{t=0}^{k}\binom{k}{t}\frac{(-1)^t r_0^\alpha}{t\tilde{r}_v^\alpha - r_0^\alpha}\Big[\prod_{x\in\Pi_\mathrm{b}\setminus\{x_0\}}\frac{1}{1+\frac{\tau_0 r_0^\alpha}{\eta}P_x\ell_x^{-\alpha}}\\ &\qquad - \prod_{x\in\Pi_\mathrm{b}\setminus\{x_0\}}\frac{1}{1+\frac{\tau_0 t\tilde{r}_v^\alpha}{\eta}P_x\ell_x^{-\alpha}}\Big], \end{aligned}\tag{45}$$

where the binomial expansion is used in the derivation. In the derivation of (45), we assume that $t\tilde{r}_v^\alpha \neq r_0^\alpha$ for $\forall t \in \{0,1,...,k\}$. Jointly considering (43) and (45), the second probability of (41) can be derived as $\mathcal{C}_2 = \mathcal{D}_1 - \mathcal{D}_2$, where

$$\begin{aligned}\mathcal{D}_1 = \binom{n}{k}\sum_{m=0}^{n-k}\binom{n-k}{m}(-1)^m\sum_{t=0}^{k}\binom{k}{t}\frac{(-1)^t r_0^\alpha}{t\tilde{r}_v^\alpha - r_0^\alpha}\\ \times \exp\big[-g(\tau_0, r_0^\alpha, m+k)\big]. \end{aligned}\tag{46}$$

In the derivation of $\mathcal{D}_1$, the PGFL of PPP is applied and the expectation over discrete random variable P is taken. Another term $\mathcal{D}_2$ is derived as

$$\begin{aligned}\mathcal{D}_2 = \binom{n}{k}\sum_{m=0}^{n-k}\binom{n-k}{m}(-1)^m\sum_{t=0}^{k}\binom{k}{t}\frac{(-1)^t r_0^\alpha}{t\tilde{r}_v^\alpha - r_0^\alpha}\\ \times \exp\big[-g(\tau_0, t\tilde{r}_v^\alpha, m+k)\big]. \end{aligned}\tag{47}$$

Combine the first probability $\mathcal{C}_1$ and second probability $\mathcal{C}_2$ of (41) and consider the probability of $\Pr\{N=n\}$, the result of (27) is obtained.

References

[1] A. Goldsmith, S. A. Jafar, I. Maric, and S. Srinivasa, "Breaking spectrum gridlock with cognitive radios: An information theoretic perspective," *Proc. of the IEEE*, vol. 97, pp. 894–914, May 2009.

[2] O. Simeone, I. Stanojev, S. Savazzi, Y. Bar-Ness, U. Spagnolini, and R. Pickholtz, "Spectrum leasing to cooperating secondary ad hoc networks," *IEEE J. Sel. Areas Commun.*, vol. 26, pp. 203–213, Jan. 2008.

[3] C. Zhai, W. Zhang, and P. C. Ching, "Cooperative spectrum sharing based on two-path successive relaying," *IEEE Trans. Commun.*, vol. 61, pp. 2260–2270, Jun. 2013.

[4] W. Su, J. D. Matyjas, and S. Batalama, "Active cooperation between primary users and cognitive radio users in heterogeneous ad-hoc networks," *IEEE Trans. Signal Process.*, vol. 60, pp. 1796–1805, Apr. 2012.

[5] S. P. Weber, X. Yang, J. G. Andrews and G. de Veciana, "Transmission capacity of wireless ad hoc networks with outage constraints," *IEEE Trans. Inf. Theory*, vol. 51, pp. 4091–4102, Dec. 2005.

[6] K. Huang, V. K. N. Lau, and Y. Chen, "Spectrum sharing between cellular and mobile ad hoc networks: Transmission-capacity trade-off," *IEEE J. Sel. Areas Commun.*, vol. 27, pp. 1256–1267, Sep. 2009.

[7] J. Lee, J. G. Andrews, and D. Hong, "Spectrum sharing transmission capacity," *IEEE Trans. Wireless Commun.*, vol. 10, pp. 3053–3063, Sep. 2011.

[8] C. Yin, C. Chen, T. Liu and S. Cui, "Generalized results of transmission capacities for overlaid wireless networks," in *Proc. IEEE International Symposium on Information Theory (ISIT)*, Seoul, Korea, Jun. 2009.

[9] M. Vu, N. Devroye, and V. Tarokh, "On the primary exclusive region of cognitive networks," *IEEE Trans. Wireless Commun.*, vol. 8, pp. 3380–3385, Jul. 2009.

[10] X. Hong, C.-X. Wang, and J. Thompson, "Interference modeling of cognitive radio networks," in *Proc. IEEE Vehicular Technology Conference (VTC Spring)*, May 11-14, 2008, pp. 1851–1855.

[11] C.-H. Lee and M. Haenggi, "Interference and outage in poisson cognitive networks," *IEEE Trans. Wireless Commun.*, vol. 11, pp. 1392–1401, Apr. 2012.

[12] R. Menon, R. M. Buehrer, and J. H. Reed, "On the impact of dynamic spectrum sharing techniques on legacy radio systems," *IEEE Trans. Wireless Commun.*, vol. 7, pp. 4198–4207, Nov. 2008.

[13] A. Rabbachin, T. Q. S. Quek, H. Shin, and M. Z. Win, "Cognitive network interference," *IEEE J. Sel. Areas Commun.*, vol. 29, pp. 480–493, Feb. 2011.

[14] A. Ghasemi and E. S. Sousa, "Interference aggregation in spectrum-sensing cognitive wireless networks," *IEEE J. Sel. Topics Signal Process.*, vol. 2, pp. 41–56, Feb. 2008.

[15] T. V. Nguyen and F. Baccelli, "A stochastic geometry model for cognitive radio networks," *The Computer Journal,* vol. 55, pp. 534–552, Jul. 2011.

[16] H. Wang, S. Ma, and T.-S. Ng, "On performance of cooperative communication systems with spatial random relays," *IEEE Trans. Commun.*, vol. 59, pp. 1190–1199, Apr. 2011.

[17] A. Bletsas, A. Khisti, D. P. Reed, A. Lippman, "A simple cooperative diversity method based on network path selection," *IEEE J. Sel. Areas Commun.*, vol. 24, pp. 659–672, Mar. 2006.

[18] B. Zhao and M. C. Valenti, "Practical relay networks: A generalization of hybrid ARQ," *IEEE J. Sel. Areas Commun.*, vol. 23, pp. 7–18, Jan. 2005.

[19] S.-R. Cho, W. Choi, and K. Huang, "QoS provisioning relay selection in random relay networks," *IEEE Trans. Veh. Technol.*, vol. 60, pp. 2680–2689, Jul. 2011.

[20] L. Xiong, L. Libman, and G. Mao, "On uncoordinated cooperative communication strategies in wireless ad-hoc networks," *IEEE J. Sel. Areas Commun.*, vol. 32, pp. 280–288, Feb. 2012.

[21] C. Zhai, W. Zhang, and G. Mao, "Uncoordinated cooperative communications with spatially random relays," *IEEE Trans. Wireless Commun.*, vol. 11, pp. 3126–3135, Sep. 2012.

[22] J. N. Laneman, D. Tse, and G. W. Wornell, "Cooperative diversity in wireless networks: Efficient protocols and outage behavior," *IEEE Trans. Inf. Theory*, vol. 50, pp. 3062–3080, Dec. 2004.

[23] Z. Sheng, Z. Ding, and K. K. Leung, "Transmission capacity of decode-and-forward cooperation in overlaid wireless networks," in *Proc. IEEE International Conference on Communications (ICC)*, Cape Town, South Africa, May 2010.

[24] Y. Xu, P. Wu, L. Ding, and L. Shen, "Capacity analysis of selection cooperation in wireless ad-hoc networks," *IEEE Commun. Letters*, vol. 15, pp. 1212–1214, Nov. 2011.

[25] R. K. Ganti and M. Haenggi, "Spatial analysis of opportunistic downlink relaying in a two-hop cellular system," *IEEE Trans. Commun.*, vol. 60, pp. 1443–1450, May 2012.

[26] J. G. Andrews, F. Baccelli, and R. K. Ganti, "A tractable approach to coverage and rate in cellular networks," *IEEE Trans. Commun.*, vol. 59, pp. 3122–3134, Nov. 2011.

[27] T. D. Novlan, R. K. Ganti, A. Ghosh, and J. G. Andrews, "Analytical evaluation of fractional frequency reuse for OFDMA cellular networks," *IEEE Trans. Wireless Commun.*, vol. 10, pp. 4294–4305, Dec. 2011.

[28] N. Jindal, S. Weber, and J. G. Andrews, "Fractional power control for decentralized wireless networks," *IEEE Trans. Wireless Commun.*, vol. 7, pp. 5482–5492, Dec. 2008.

[29] C. Zhai, H. Xu, J. Liu, L. Zheng, and Y. Zhou, "Performance of opportunistic relaying with truncated ARQ over Nakagami-m fading channels," *Trans. Emerg. Telecomms. Techs.*, vol. 23, pp. 50–66, Jan. 2012.

[30] G. Mao, B. Fidan, and B. Anderson, "Wireless sensor network localization techniques," *Computer Networks*, vol. 51, pp. 2529–2553, Jul. 2007.

[31] F. Baccelli, B. Blaszczyszyn, and P. Muhlethaler, "An aloha protocol for multihop mobile wireless networks," *IEEE Trans. Inf. Theory*, vol. 52, pp. 421–436, Feb. 2006.

[32] D. Stoyan, W. Kendall, and J. Mecke, *Stochastic Geometry and Its Applications*, 2nd Edition. New York: Wiley, 1996.

[33] M. Haenggi and R. K. Ganti, "Interference in large wireless networks," *Foundations and Trends in Networking (NOW Publishers)*, vol. 3, pp. 127–248, 2008.

[34] H. S. Dhillon, T. D. Novlan, and J. G. Andrews, "Coverage probability of uplink cellular networks," in *Proc. IEEE Global Communications Conference (GLOBECOM)*, Anaheim, California, USA, Dec 3-7, 2012, pp. 2203–2208.

[35] I. S. Gradshteyn and I. M. Ryzhik, *Talbe of Integrals, Series, and Products*, 7th Edition. Academic Press, 2007.